

REPORT DOCUMENTATION PAGE

Form Approved
OMB NO. 0704-0188

Public Reporting burden for this collection of information is estimated to average 1 hour per response, including the time for reviewing instructions, searching existing data sources, gathering and maintaining the data needed, and completing and reviewing the collection of information. Send comment regarding this burden estimates or any other aspect of this collection of information, including suggestions for reducing this burden, to Washington Headquarters Services, Directorate for information Operations and Reports, 1215 Jefferson Davis Highway, Suite 1204, Arlington, VA 22202-4302, and to the Office of Management and Budget, Paperwork Reduction Project (0704-0188,) Washington, DC 20503.

1. AGENCY USE ONLY (Leave Blank)		2. REPORT DATE 2-21-07	3. REPORT TYPE AND DATES COVERED Final report, 9/10/03 - 9/9/06	
4. TITLE AND SUBTITLE Uncovering Design Principles of Intermediate Filaments, a Self-Assembling Biomaterial: Lessons in Nanoscale Materials			5. FUNDING NUMBERS DAAD19-03-1-0330 Design	
6. AUTHOR(S) David H. Lee				
7. PERFORMING ORGANIZATION NAME(S) AND ADDRESS(ES) Tufts University, Dept. of Chemistry, 62 Talbot Ave. Medford, MA 02155			8. PERFORMING ORGANIZATION REPORT NUMBER A140001-ARM205	
9. SPONSORING / MONITORING AGENCY NAME(S) AND ADDRESS(ES) U. S. Army Research Office P.O. Box 12211 Research Triangle Park, NC 27709-2211			10. SPONSORING / MONITORING AGENCY REPORT NUMBER 44457-LS 4 4 4 5 7 . 3 - L S	
11. SUPPLEMENTARY NOTES The views, opinions and/or findings contained in this report are those of the author(s) and should not be construed as an official Department of the Army position, policy or decision, unless so designated by other documentation.				
12 a. DISTRIBUTION / AVAILABILITY STATEMENT Approved for public release; distribution unlimited.			12 b. DISTRIBUTION CODE	
13. ABSTRACT (Maximum 200 words)				
14. SUBJECT TERMS bionanotechnology, self-assembly, protein design, virus, collagen			15. NUMBER OF PAGES	
			16. PRICE CODE	
17. SECURITY CLASSIFICATION OR REPORT UNCLASSIFIED	18. SECURITY CLASSIFICATION ON THIS PAGE UNCLASSIFIED	19. SECURITY CLASSIFICATION OF ABSTRACT UNCLASSIFIED	20. LIMITATION OF ABSTRACT UL	

NSN 7540-01-280-5500

Standard Form 298 (Rev.2-89)
Prescribed by ANSI Std. Z39-18
298-102

I. Statement of Problem Studied

Our broad long-term objective is to create novel biomaterials that advance the technical capabilities of the U.S. Army. In the short term, we seek to design self-assembling biomaterials that are adaptable in their structure and function. To do so, we must understand the molecular physicochemical aspects of biomaterials design, and we use three different systems to study this issue: 1) intermediate filaments, a class of protein with a broad range of structural roles from the nanometer to macroscale, as a model system; (2) self-assembled virus-based nanostructures, and (3) adiponectin, an adipocyte-produced hormone that serves as a soluble model system of higher order collagen. Such proteins may be harnessed for military purposes (eg. protective self-healing materials or nanoscale scaffolds) if one had a better understanding of how molecular structure determines material properties. In this final progress report, we summarize our studies on these systems.

II. Technical Summary

1. Intermediate Filament Engineering:

Figure 1 shows our scheme for engineering the intermediate filament vimentin into a soluble model system. Intermediate filaments (IFs) are structural proteins that can be parsed into head and tail globular domains separated by a long coiled-coil rod region. This monomer first goes on to form dimers followed by higher order oligomerization. It has been established that specific regions of rod domain interact in this process [1-3]. Given that coiled-coil structure, a motif whose design principles are well understood, comprises this region, it may be possible to permute this domain to redirect assembly of the wild type polypeptide rod. Figure 1 illustrates steps by which IFs are believed to assemble. Interestingly, the two staggered dimer of dimers in step 2 are "reciprocal" structures. These two staggered arrangements ensure an indefinite perpetuation of lengthwise association, giving rise to the filament (much like DNA duplexes with sticky ends). However, if one were to permute the rod by moving the overhang portion of the coiled-coil from one end to the other, one would in principle, preserve all native interactions in the oligomer, but eliminate the overhang that gives rise to length-wise growth of the filament and the formation of alternate structures. Most importantly, lateral interactions between oligomers should not be affected since the vast majority of native interactions remain (with the exception of the new "splice" site). Previous evidence shows that at Lys282 can form intermolecular cross-links with both Lys104 and Lys402. Thus, any construct we make must place Lys 104 and Lys 402 in close proximity[1-3]. Knowing that the rod must be α -helical over most of its length, the number of constructs possible is drastically reduced upon inspection of the various sequences in the context of a helical wheel diagram (Figure 2). Only constructs that place Lys 104 and Lys 402 3, 4 or 7 residues apart can position the two residues close in space. Note that the head and tail have been removed from the engineered and wild type sequences to abrogate elongation and alternate structures. If the heteromer undergoes full assembly, the expected complex should have the side-to-side bundling characteristics of a normal IF but have a discrete length of a single rod domain! Such a discrete particle would be much more amenable to biophysical characterization than an indefinitely long filament.

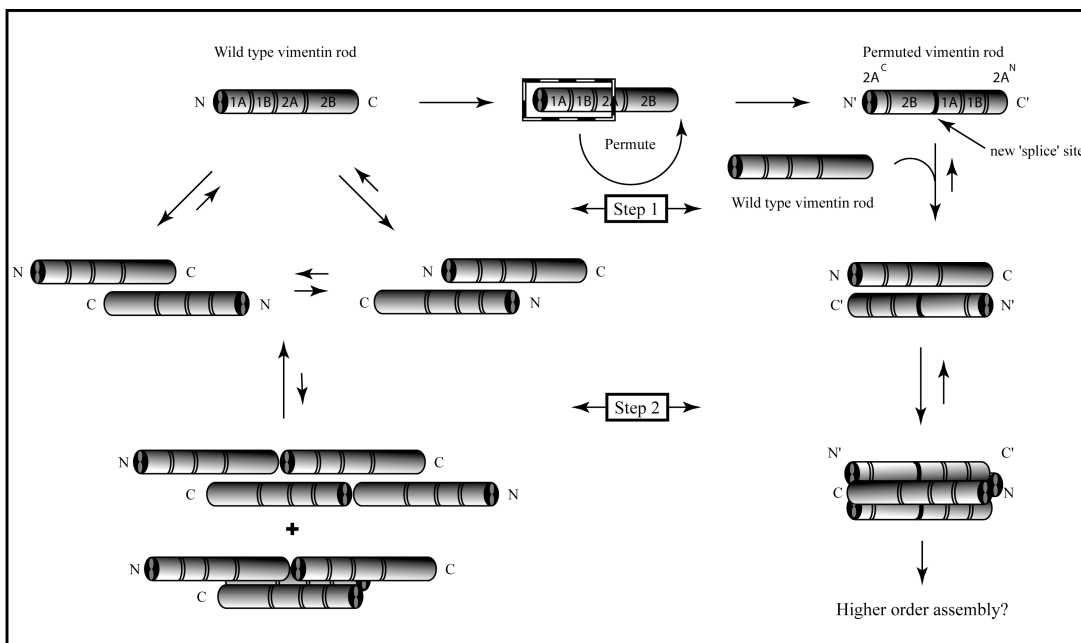


Figure 1. Assembly of wild type vs. permuted vimentin rod domains. The dimeric coiled-coil segments 1A, 1B, 2A, and 2B are represented as a cylinder while the double lines depict linker regions. The amino- and carboxy termini are marked as N and C respectively. *Left:* Assembly of wild type rod domains leads to 2 reciprocal antiparallel tetramers in step 1 that have open binding sites, leaving open the possibility of forming alternate higher order structures. Without the head domain however, the tetramer form is greatly favored. *Right:* Assembly of a permuted vimentin rod with the wild type sequence is expected to lead initially to a dimer of coiled-coils (tetramer) that has the binding sites from the overhang regions completely satisfied, thus permitting only lateral growth. This new complex is expected to assemble to at least the tetramer stage. In principle, tetramers may further assemble to form a tetramer of tetramers, which would represent a cross-section of a fully assembled intermediate filament (not shown). The thick line demarcates the new 'splice' site. N' and C' signify the new termini of the permuted polypeptide. Also, in the permuted rod, coiled coil 2A was split, so the carboxy and amino terminal halves are distinguished with 'C' and 'N' respectively.

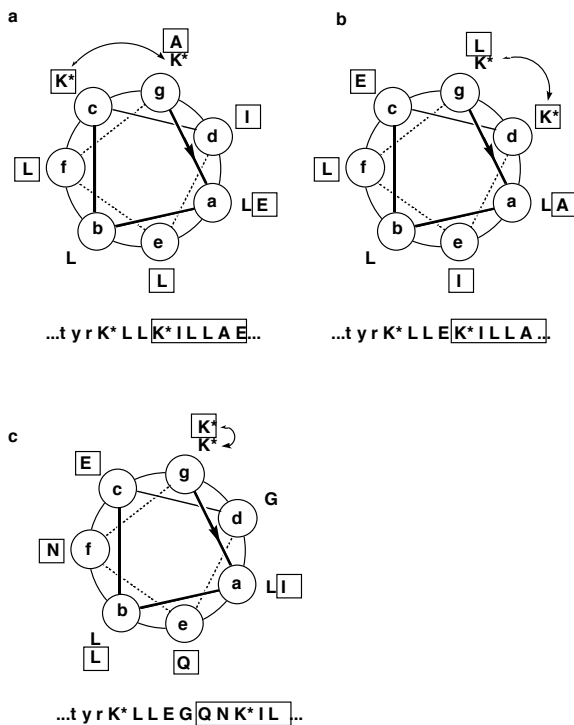


Figure 2. Helical wheel diagrams of the three permuted rod constructs made for this project: a) 12.4, which places the two lysines 4 residues apart (b) 12.5, which places the two lysines 3 residues apart; (c) 12.6, which places the two lysines 7 residues apart.

The 3 constructs were made by splicing the two relevant halves together by overlap extension. This was not as straightforward we initially believed but we were able to obtain all three and verified their correctness by sequencing. An unexpected point mutation was corrected by site-directed mutagenesis after cloning into the pET3d expression vector. Following transformation into BL21 strain of *E. coli*, construct 12.6 was overproduced. We can achieve approximately 11 mg/L of culture and we are currently optimizing expression conditions for 12.4 and 12.5. Construct 12.6 was purified by ion exchange chromatography on DEAE resin using 20 mM Tris at pH7, 6M urea as the base buffer. The protein eluted at 150 mM NaCl.

The CD spectrum of 12.6 was obtained to ascertain that it was at least helical, a sign that it was adopting the coiled-coil conformation. Shown in Figure 2 is its CD spectrum. It shows that 12.6 is likely to have coiled-coil structure as the $\theta_{222}/\theta_{208}$ ratio is 0.93, in line with that measured for many coiled-coils. The positive CD signal at near UV wavelengths, a contribution of aromatic residues in certain configurations, is prominent here but absent in the CD spectrum of the wild type protein, suggesting that the construct may not have a fully native structure. We conclude that this construct either has some non-helical structure or is not fully associated and may display some concentration dependence in its association.

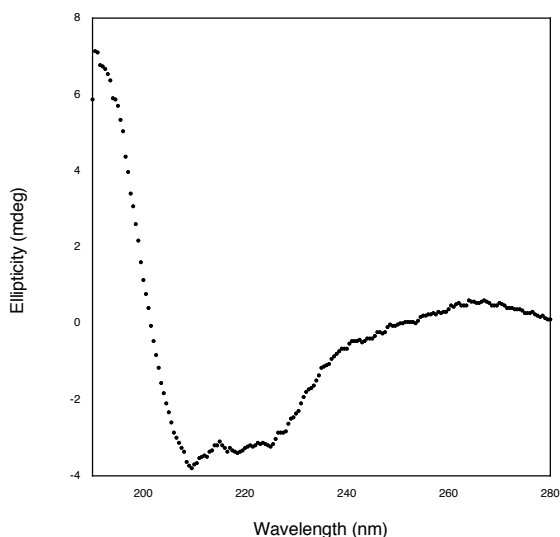


Figure 2. Circular dichroism spectrum of permuted construct 12.6. The shape of the spectrum suggests that the protein has coiled-coil structure but is not fully helical, and has regions of structure that are indeed different that wild type, given the positive signal at near UV wavelengths.

We have purified the other constructs and mixed them with the wild type rod to see if we can obtain soluble oligomers that are suitable for biophysical analysis. Each construct has very low solubility, even under denaturing conditions, (eg. 4 M urea). We have attempted to refold them in the presence of the wild type rod but most of the protein still precipitated. Nevertheless, transmission electron micrographs of the suspension showed the presence of large rod-like structures (Figure 1). The diameters are highly uniform but there is heterogeneity with regards to its length.

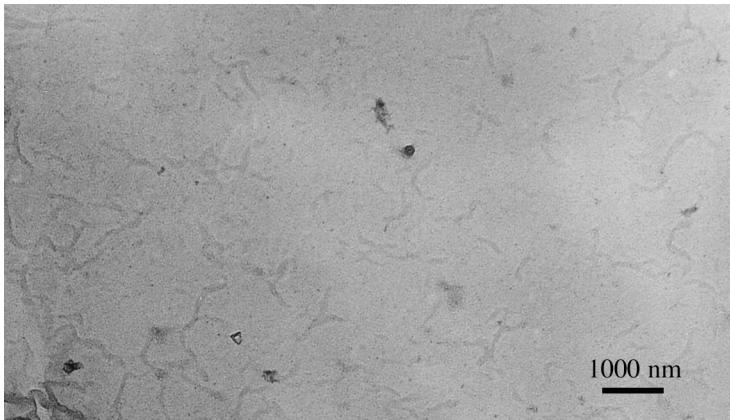


Figure 3. Transmission electron micrograph of vimentin rod assemblies. Wild type vimentin rods were mixed with domain-swapped construct 12.6 and dialysed into reassembly buffer. Imaging the supernatant revealed the presence of large worm-like structures.

2. Self-Assembly of a Linear Viral Array:

The goal of this project is to use TMV as a nanoscale building block to create novel structures and devices. TMV is an ideal system to start with because is the best studied virus, and is very simple in its composition and structure. It is made up of a 6395 nucleotide single stranded RNA that is encapsulated by 2130 copies of a single type of coat protein [4]. The final structure is a 300 nm long rod, with an 18 nm diameter. Virus assembly is dictated by a 68 nucleotide packaging signal (called the origin of assembly, OAS) [5,6], and any RNA that bears this signal gets packaged by the coat protein. A consequence of packaging foreign RNA however, is that the resultant length of the viral pseudoparticle is determined by the length of the RNA! We are exploiting these decades-old *in vitro* assembly properties in combination with modern molecular biology techniques and oligonucleotide modification chemistry to create highly ordered 1-dimensional arrays. The overarching concept is to create TMV pseudovirions that have a biotin group on both ends of the particle, then use streptavidin to organize the TMV into a linear array (Figure 4).

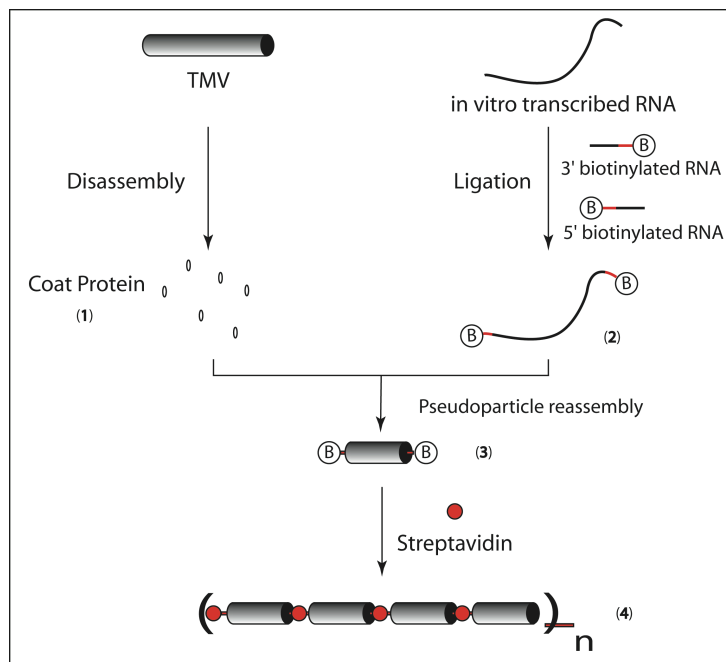


Figure 4. Strategy for assembling a linear viral array. Coat protein (1) was isolated from TMV and used to package 5', 3' bis-biotinylated RNA (2) to form a pseudoparticle (3) whose length is determined by (2). The pseudoparticle self-assembles with streptavidin to form the linear array (4). The RNA was biotinylated by ligating synthetic RNAs bearing a biotin (B) attached to either the 5' or 3' end via a 5 nm PEG linker (red). Objects are not drawn to scale.

The high affinity of streptavidin for biotin, on the order of 10^{14} M^{-1} , is well known and should assure a high degree of assembly. Streptavidin is a tetramer, and thus should be able to organize up to 4 TMV particles. The domain structure is that of a dimer of antiparallel dimers. The 4 binding sites for biotin have a tetrahedral relationship. The 18 nm diameter of TMV, being three times larger than streptavidin however, imposes steric constraints on the spacing between the biotin group and the end of the virus such that the linker spacing will determine whether it assembles as a linear array or some higher order structure. As shown in Figure 5, a short linker permits binding of only two TMVs to tetrameric streptavidin at 180 degrees relative to each other. Thus, streptavidin is arrayed in a regular linear fashion by TMV and has two remaining binding sites available to array other biotinylated objects. Third, the high affinity for biotin will be a great driving force for high yields in assembly with stoichiometric amounts of TMV and streptavidin.

This system is significant because the tunability of its dimensions along with the ability to chemically or genetically modify the virus and/or streptavidin enables assembly of nanostructures with diverse function and size, making it potentially amenable to a wide range of applications in nanoscience. In particular, the enzymatic production of RNA enables the assembly of long pseudoparticles that would exceed the 100 nm length scale that borders the focus of nanoscience, in addition to the sub 100 nm regime we are currently exploring. Furthermore, TMV is much more rigid than nucleic acids, and so in addition to the size scale accessible to self-assembled bionanosystems, this system nicely may yield structures with materials properties that are advantageous with respect to what has been achieved with nucleic acids.

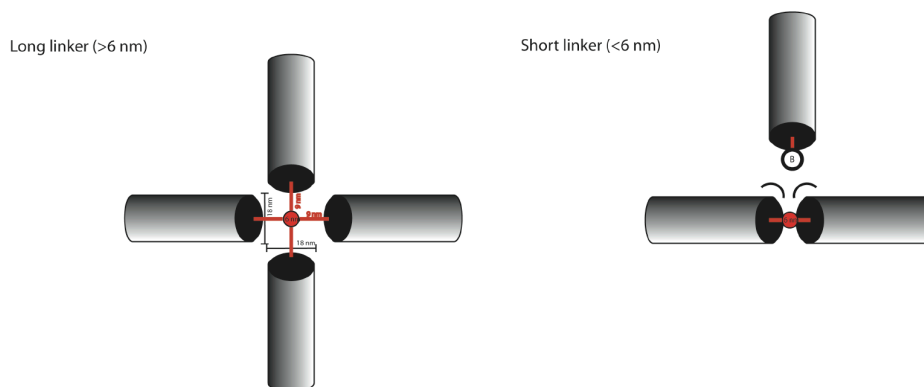


Figure 5. Influence of linker length on the structure of streptavidin-virus assembly.

Long linkers joining the bioint to the RNA are required for 4 18 nm diameter viral particles to assemble around the 6 nm diameter streptavidin (top). Short linkers permit end to end interactions while alternative approaches are excluded by the steric influence of particles already bound to streptavidin. We use 5 nm linkers to direct assembly to the 1D structure.

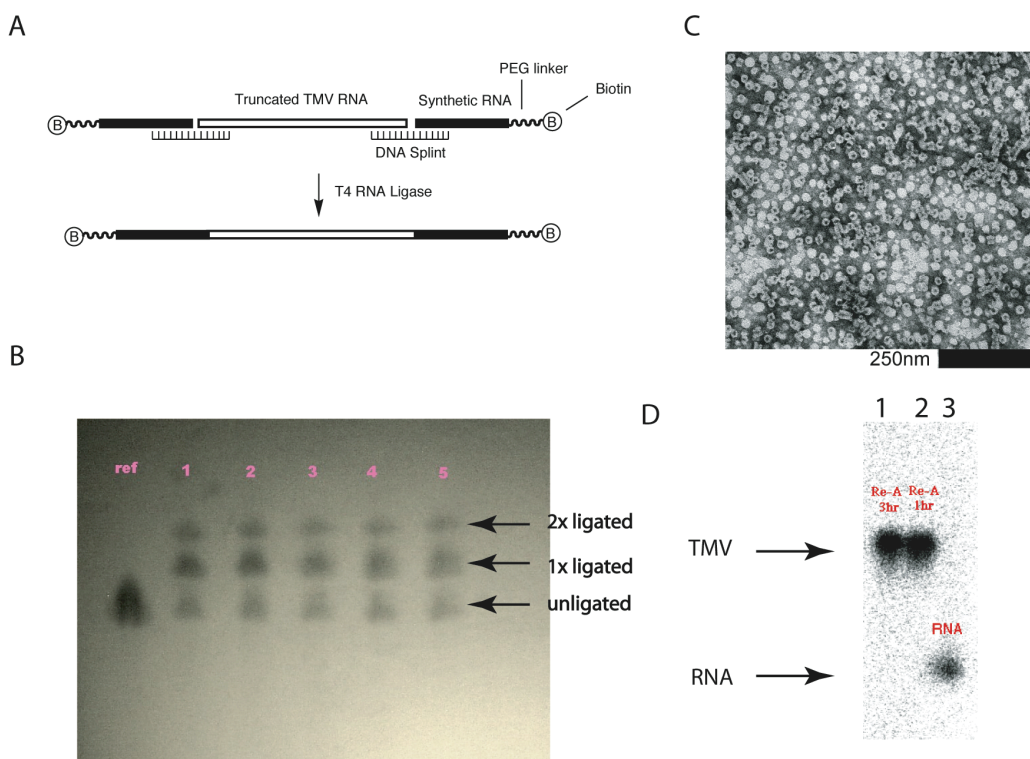


Figure 6. Production of TMV pseudoparticle components. *A.* Schematic of the splinted ligation. T4 DNA ligase catalyzes the ligation of TMV RNA (white segment) and the synthetic biotinylated RNA (black segment) via a DNA splint. The sequence specificity of the reaction permits ligation of 2 synthetic RNAs simultaneously. *B.* Polyacrylamide gel of 5 splinted ligation reaction products as visualized by UV backshadowing. *C.* Transmission electron micrograph of coat protein at 1mg/mL. Note the disk shaped morphology with the open channel in the center. *D.* Autoradiogram of a coat protein/³²P RNA reassembly reaction. Lane 1 and 2: RNA / coat protein reassembly reaction after 3 hours and 1 hour respectively; Lane 3: Unpackaged reference RNA.

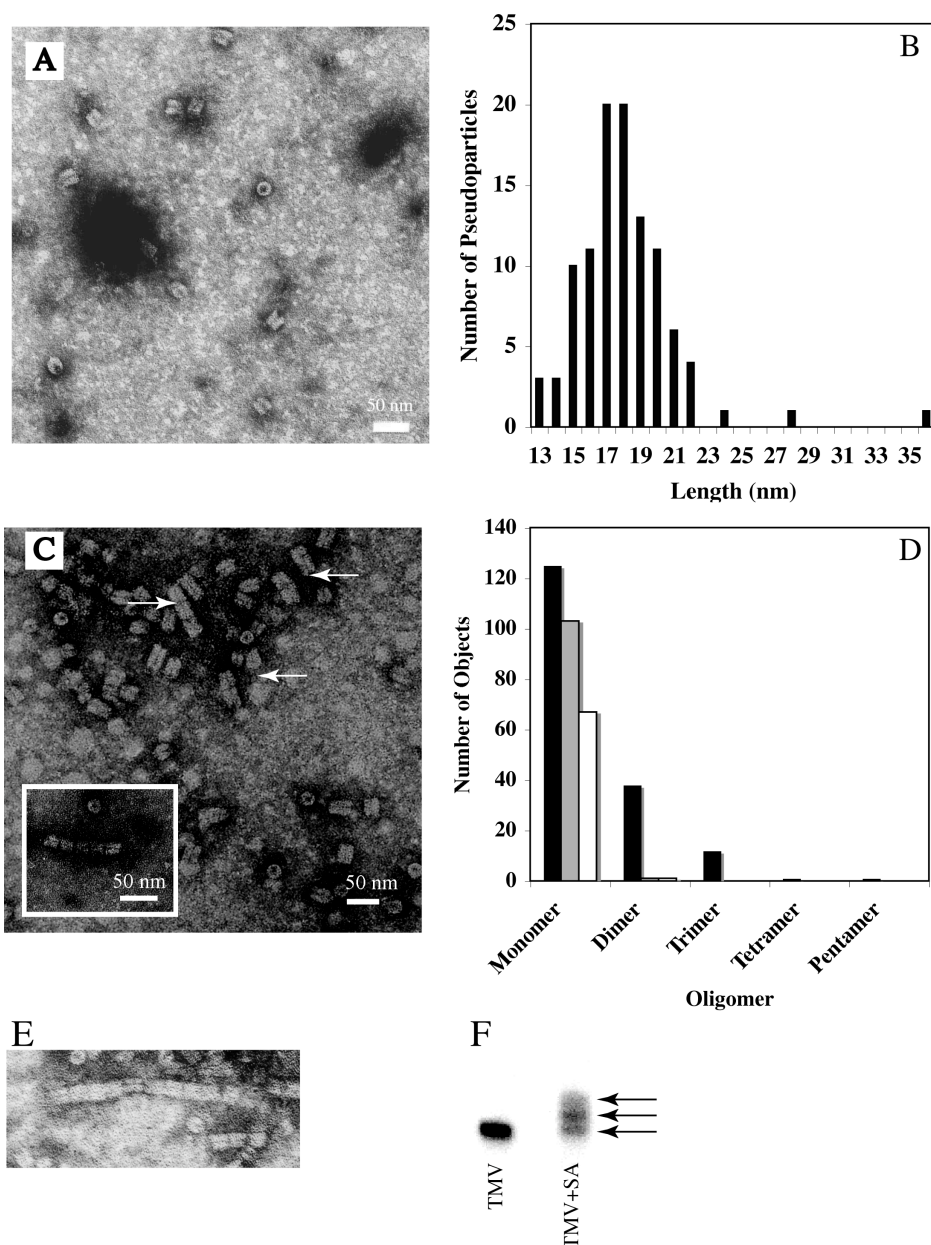


Figure 7. Characterization of TMV arrays. a) Transmission electron micrograph of doubly biotinylated pseudoparticles which are monodisperse in the absence of streptavidin. (b) Statistical analysis of monomeric pseudoparticle length from 4 fields of view. Most particles have the expected length of 17 nm. (c) Transmission electron micrograph of pseudoparticles from (a) mixed with an equimolar amount of streptavidin tetramer after 30 minutes. Trimers and dimers are evident. Inset: 1 of several pentamers observed after 30 minutes (d) Statistical analysis of the TMV/streptavidin self-assembly reaction after 30 minutes (black) and the negative controls where either streptavidin (grey) or biotin (white) are missing. Dimers and higher order assemblies were evident in 10 fields of view. The negative control contained predominantly monodisperse particles with several dimers present. (e) Nonamers become more prevalent after 2 hours of assembly. In (f) the formation of multimers of TMV was revealed by autoradiography with electrophoretic separation. Discernable bands are from arrays having different numbers of pseudoparticles.

The convergent strategy uses well-established methods at each step (Figure 6). The coat protein is isolated by Fraenkel-Conrat's acetic acid method [7-9]. 322 Nucleotide long RNA containing the OAS was obtained by in vitro transcription of RT-PCR products of TMV RNA. We ligate the synthetic RNAs to these transcripts by DNA-splinted ligation. Packaging of the RNA yields a bis-biotinylated 18 nm rod. This rod can be assembled into short arrays by addition of an equimolar amount of streptavidin. Shown in Figure 7 are transmission electron micrographs of the single particles and the arrays formed after addition of streptavidin. In the absence of streptavidin, the particles are monodisperse. 30 minute exposure to streptavidin however, causes the pseudoparticles to assemble into dimers, trimers, and in rare cases, tetramers and pentamers.

After only 30 minutes, only half of all pseudoparticles observed were participating in array formation and most of them were short, being dimers and trimers. These short arrays were formed after only 30 minutes and so we let the assembly process proceed for longer periods. We observed some longer structures, such as the nine membered array shown in Figure 7E but most of the arrays were still 2-3mers, and the majority of viral particles remained monomeric.

...ABABABABABABABAB...

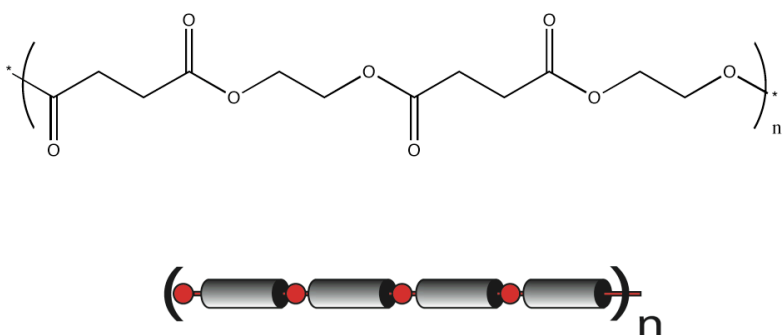


Figure 8. A comparison of an alternating copolymer with a viral array.

The shortness of the arrays can be rationalized through consideration of step growth polymer mechanisms. Shown in Figure 8 is a comparison of the linear viral array with a polyester, a representative alternating copolymer. Both are built from an alternating pattern of monomers. The length of alternating copolymers (reflected in the degree of polymerization, DP) can be related to the extent of the reaction, p, by the classical Crother's Equation

$$DP = [\text{initial \# of functional groups}] / [\text{\# of groups after time } t] = 1/(1-p) \quad (1)$$

Shown in Table 1 are some calculated values of DP for various p. At p=0.5 (50% completion of reaction or assembly) where only half of the pseudoparticles are in arrays, the DP=2. This is reflective of a very short polymer and possibly explains why we observed mostly dimers and trimers. Table 1 also shows how difficult it is to created

alternating copolymers of substantial length: at 95% completion ($p=0.95$), $DP=20$. This outcome does not necessarily diminish the importance of making viral arrays however, as the desired length will be dependent upon the application of array.

Table 1. Dependency of Degree of Polymerization on Extent of Reaction

Extent of Reaction, p	Degree of Polymerization
0.5	2
0.9	10
0.95	20
0.99	100
0.999	1000
1	infinity

To gain additional insight into the formation of arrays of different length, we are currently developing electrophoretic methodology to make quantitative measurements on each array. Shown in Figure 7F are some promising preliminary results where we electrophoresed ^{32}P -radiolabelled TMV arrays on an agarose gel. While the separation of the individual arrays needs to be greatly improved, individual bands may be discerned in the smear that is formed upon assembly with streptavidin.

3. Higher Order Structure of Adiponectin a Soluble Model System of Collagen Interactions:

Collagen is a structural protein is the principle component of the extracellular matrix that provides mechanical support to connective tissues such as skin, tendon, ligament, bone and cornea [10]. It is characterized by a Gly-X-Y repeat of amino acids which folds into a polyproline-like helix that trimerizes to form a three stranded superhelix. This triple helix goes on to self-assemble across multiple length scales to form organized suprafibrillar structures that determine the mechanical and biological properties of the tissue. For example, collagen fibrils are organized in a concentric manner in bone to provide resistance to compression forces [11] while the crimped morphology in tendon permits elasticity [12,13]. Thus, gaining an understanding of the design principles of higher order collagen structure would greatly enhance our understanding of its function in biology, facilitate the design of biomaterials, and perhaps find novel applications in bionanotechnology, where exquisite structural control at the nanoscale is often required.

At present, there is a gap in our knowledge regarding the relationship between collagen sequence and how it influences higher order assembly. At the molecular level, an extensive body of work on the thermodynamic stability, folding and structure of collagen triple helices exists has been built up based on model peptides. For example, the thermodynamic propensities of the twenty amino acids at the X and Y positions have been determined in the context of a host Gly-Pro-Hyp collagen triple helix [14]. Sequence variation has also been shown to cause changes in the helical parameters of the triple helix [15]. The role of hydration [16], the stabilizing feature of 4-hydroxyproline (Hyp) [17,18], as well as the effect of electron withdrawing groups at the 4- position on the conformational preferences of proline [19-22] have also been characterized. Collagen suprafibrils have also been extensively studied. Notably, it has been shown that in fibrils,

triple helices are packed into quasihexagonal three-dimensional crystalline arrays with a left-handed twist [23]. While short and simple model peptides have been shown to undergo higher order assembly [24-26] or form liquid crystals [26], how unique collagen sequences lead to specific higher order structures is unknown.

The study of higher order collagen assembly is complicated by several factors. First, collagens often need chaperones to assist in their folding. This requirement limits the sequences that can be tested for their assembly properties *in vitro*. Second, non-collagenous domains are often involved in higher order assembly as well [27]. These globular domains and telopeptides vary widely in sequence from one collagen to the next so it is difficult to generalize from individual studies, and the nature of the telopeptide-collagen interactions at the atomic level is unknown. Third, collagens undergo glycosylation [28-30], particularly with glucosylgalactosyl moieties at sites having 5-hydroxylysyl residues. These disaccharides may be important for higher order assembly but is difficult to recapitulate *in vitro*. Fourth, covalent cross-links, such as disulfide bonds, are often important for higher order structures [31]. Where these should be incorporated into a collagen containing protein is unknown but they often occur in the non-collagenous regions. Fifth, self-assembly often leads to insolubility in the higher order structures that are formed [32]. This insolubility limits the biophysical experiments that are usually carried out to determine oligomeric structure and thermodynamic interactions. Thus, in order to determine the roles played by these additional features of collagens, a soluble model system having these traits and that is amenable to systematic variation is required.

The hormone known as adiponectin (as well as Acrp30, APM1, GBP28, or AdipoQ) may be a suitable protein to use as a model system to explore higher order collagen interactions. Adiponectin is a 30 kDa C1q-like protein that contains a perfect 22 Gly-X-Y collagen-like repeats sandwiched between a 17 residue N-terminal domain and a globular C-terminal domain that is structurally similar to TNF- α (see Figure 9). Thus, the domain organization is similar to that of collagen X. It is secreted exclusively by adipocytes in multiple homomeric oligomers that we and Lodish previously determined to be a trimer, a hexamer, and a "high molecular weight complex" [33,34]. Furthermore, we and Lodish, along with others established that the N-terminal domain contains a single cysteine residue that is critical to mediating adiponectin oligomerization through disulfide bond formation [33]. As such, these oligomers do not spontaneously equilibrate. Despite multiple efforts [35,36], no biological mechanism for interconversion has been found either. Like most collagens, adiponectin is post-translationally modified with glucosylgalactosyl groups at conserved 5-hydroxylysine residues in the collagen-like domain (four in total) [37-39]. These disaccharides have been shown to be required for formation of the HMW complex as their mutation led to the loss of this oligomer in transiently transfected cells [37-39]. Similarly, recombinant adiponectin expressed in *E. coli*, which gives unglycosylated protein, fails to form HMW oligomers and is likely misfolded [34]. Though not N-glycosylated [37], it is also likely that adiponectin is O-glycosylated with more complex polysaccharides on threonine residues in the collagen-like domain [40]. Thus, in light of the fact that adiponectin has similar domain organization as some collagens, is glycosylated as a typical collagen would be, forms a

soluble complex and homomeric (which simplifies analysis, compared to heteromeric C1q for example), we are exploring its utility as a model system for microfibrillar collagen assembly. As a first step towards this goal, we carried out structural analyses of HMW adiponectin.

Sedimentation equilibrium experiments were carried out to define the molecular weight of the complex [41]. All sedimentation equilibrium experiments, carried out at 5000 rpm and 6000 rpm at 10 μ M and 1 μ M respectively, were consistent with HMW adiponectin being an octadecamer. Shown in Figure 10C is a typical trace obtained at 5000 rpm, along with residuals. All data sets fit best to an ideal single species model with random residuals (top). The random residuals provide further evidence that the sample is not undergoing measurable equilibrium with other oligomeric states. The apparent molecular weight, calculated from the average of 10 experiments, was determined to be 485 968 kDa, 18.4 \pm 1.1 times larger than the glycosylated monomer (26 455 Da). We conclude that HMW adiponectin is an octadecamer.

Dynamic light scattering measurements gives additional data regarding the hydrodynamic size of the bovine complex [41]. The autocorrelation function, shown in Figure 10A, is monoexponential as determined by the method of cumulants [42], with random residuals, indicating that it is monodisperse and that there are no other physical processes that are occurring at detectable levels. The apparent hydrodynamic radius extracted from the autocorrelation function centers on 9.0 nm (Figure 10B). Using the calculated mass of octadecameric adiponectin, the theoretical size of an anhydrous 485 968 Da sphere is however estimated to be only 5.2 nm [43]. Thus HMW adiponectin is asymmetric, which is expected if it were C1q-like in structure. From the Stoke-Einstein equation, the ratio of f / f_0 is 1.73. Modeled as an oblate ellipsoid, bovine HMW adiponectin has a maximal axial ratio = 11.8 with the long axes (2a) of the hydrated form being 26.8 nm in length and the short axis (2b) is 2.3 nm. The short axis seems unrealistically small but such an outcome was also obtained for C1q [44]. The long axes of the ellipsoid were comparable to the diameter of the splayed complexes observed by electron microscopy (2a=33 nm) but the short axis (2b) was a mere 2.2 nm in length. Thus, HMW adiponectin seems to have similar hydrodynamic behavior to C1q.

The bouquet-like objects (Figure 11) observed for bovine HMW adiponectin by TEM [41] provide additional insight into the structure of HMW adiponectin beyond prior EM studies [33,36]. First, it is clearly reminiscent of C1q [45,46]. In flattened side views (bottom row), six globular objects can be seen atop thin stalks, which presumably correspond to the 6 trimers on collagen triple helices that are required to form the octadecameric complex. The stalks bunch together at the other end in a manner that is consistent with the requirement for N-terminal disulfide bonding [33,47,48]. While the disulfide-bond pattern of the complex remains to be elucidated, the overall architecture of HMW adiponectin is highly similar to C1q.

Some of the side views of HMW adiponectin (Figure 11, middle row) suggest a conical structure of the oligomer with the C-terminal portion forming the base. Interestingly, these globular domains are arranged in a tight ring. End-on views of the

complex (Figure 11, top row) also show this arrangement, although some structures formed a circle of 5 globular domains plus one in the middle. The N-terminal region of the collagen domains sometimes appeared to be bundled together, implying higher order collagen interactions. Presumably, these interactions help direct the subunits to be parallel and form a closely packed cone,

Tangential to the goal of this project is the great interest in measuring oligomer distribution in serum as there is evidence that different oligomers have different metabolic activities. We have developed a rapid ion-exchange protocol that permits separation of the complexes, probably through differences in polyvalency. Shown in Figure 12 is a western blot highlighting the effectiveness of our methodology in separating adiponectin oligomers from cell culture media of 3T3-L1 adipocytes. Each oligomer can be specifically eluted with buffer containing an appropriate concentration of NaCl.

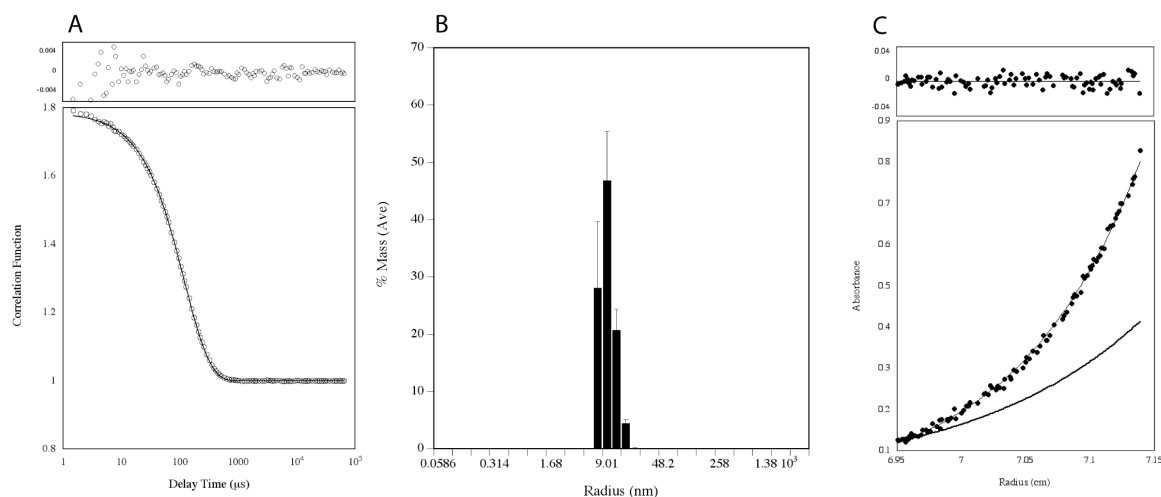


Figure 10. Biophysical characterization of endogenous HMW adiponectin. A. The autocorrelation function obtained by dynamic light scattering for bovine HMW adiponectin (circles) was fit by the method of cumulants and showed monoexponential decay, indicating a monodisperse sample. Residuals are shown above. B. The Stokes radius that was calculated from this curve centered on 9 nm. C. Sedimentation equilibrium trace of bovine HMW adiponectin. Data points (circles) were fit to an ideal single species model having an apparent molecular weight of 482 kDa, or 18 times the monomer. The residuals are shown above. For reference, a theoretical trace for a dodecamer (bold curve) is shown.

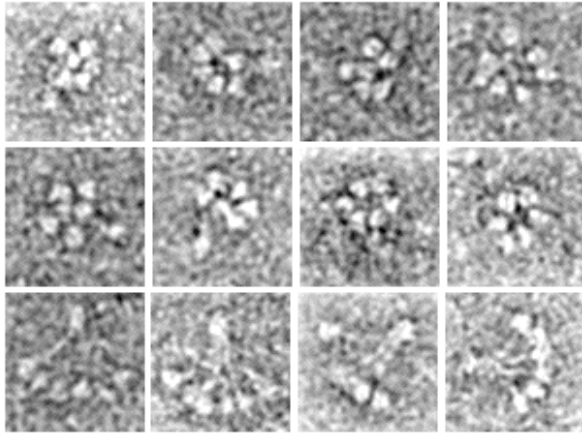


Figure 11. A montage of transmission electron micrographs of high molecular weight adiponectin. The bottom row depicts side views of the complex highlighting its C1q-like structure. The images contain 5-6 “heads”, presumably reflecting the trimeric globular domains that make up the octadecameric assembly.

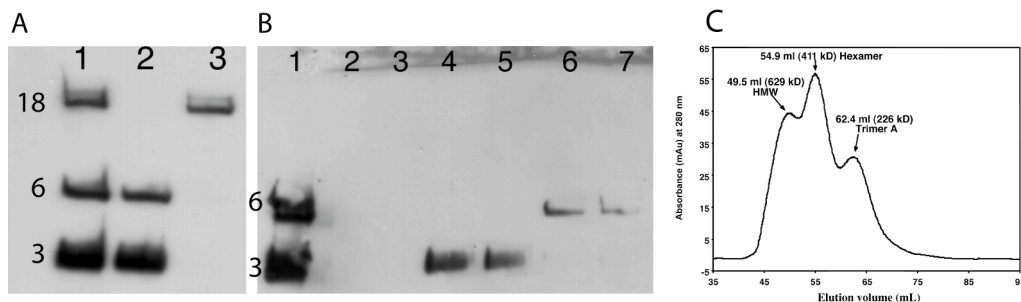


Figure 12. Purification of HMW adiponectin. A. Conditioned media from 3T3-L1 adipocytes (lane 1) was chromatographed on ion-exchange resin. The unbound fraction (lane 2) contains the trimer (3) and hexamer (6) while the HMW (18, lane 3) eluted under high salt conditions. B. The trimer and hexamer from the flow through of A (lane 1) could also be individually eluted by step washing an ion-exchange column. C. For comparison, the elution profile of adiponectin oligomers from a Superdex 200 gel filtration column is shown. Reproduced from our publication in [33].

III. Summary of Most Important Results

1. Permuted vimentin rod domains could self-assemble into fibrils of defined diameter.
2. Tobacco mosaic virus could be engineered to form pseudoparticles of controlled length and with chemo- and regiospecific functionalization to yield nanorods that could be assembled with streptavidin into linear arrays.
3. The structure of high molecular weight adiponectin was established. This soluble model system paves the way for the study of determinants of higher order collagen assembly.

IV. Bibliography

- [1] Steinert, P.M., Marekov, L.N. and Parry, D.A.D. (1993) Diversity of Intermediate Filament Structure: Evidence that the Alignment of Coiled-Coil Molecules in Vimentin is Different from that in Keratin *Journal of Biological Chemistry* 268, 24916-24925.

REPORT DOCUMENTATION PAGE (SF298)
(Continuation Sheet)

- [2] Steinert, P.M., Marekov, L.N., Fraser, R.D.B. and Parry, D.A.D. (1993) Keratin Intermediate Filament Structure: Crosslinking Studies Yield Quatitative Information on Molecular Dimensions and Mechanism of Assembly *Journal of Molecular Biology* 230, 436-452.
- [3] Steinert, P.M., Marekov, L.N. and Parry, D.A.D. (1999) Molecular Parameters of Type IV α -Internexin and Type-IV-Type III α -Internexin-Vimentin Copolymer Intermediate Filaments *Journal of Biological Chemistry* 274, 1657-1666.
- [4] Namba, K. and Stubbs, G. (1986) Structure of tobacco mosaic virus at 3.6 Å resolution: implications for assembly *Science* 231, 1401 - 1404.
- [5] Butler, P.J.G. (1999) Self-assembly of tobacco mosaic virus: the role of an intermediate aggregate in generating both specificity and speed *Phil. Trans. R. Soc. Lond. B* 354, 537 - 550.
- [6] Turner, D.R., Joyce, L.E. and Butler, P.J.G. (1988) The tobacco mosaic virus assembly origin RNA (Functional characteristics defined by directed mutagenesis) *J. Mol. Biol.* 203, 531 - 547.
- [7] Fraenkel-Conrat, H. and Singer, B. (1999) Virus reconstitution and the proof of the existence of genomic RNA *Phil. Trans. R. Soc. Lond. B* 354, 583 - 586.
- [8] Fraenkel-Conrat, H. (1957) Degradation of tobacco mosaic virus with acetic acid *Virology* 4, 1 - 4.
- [9] Fraenkel-Conrat, H. and Williams, R.C. (1955) Reconstitution of Active Tobacco Mosaic Virus Fromits Inactive Protein and Nucleic Acid Components *Proc. Natl. Acad. Sci. USA* 41, 690-698.
- [10] Wess, T.J. (2005) Collagen fibril form and function *Adv Protein Chem* 70, 341-74.
- [11] Diamant, J., Keller, A., Baer, E., Litt, M. and Arridge, R.G. (1972) Collagen; ultrastructure and its relation to mechanical properties as a function of ageing *Proc R Soc Lond B Biol Sci* 180, 293-315.
- [12] Wess, T.J., Hammersley, A.P., Wess, L. and Miller, A. (1998) Molecular packing of type I collagen in tendon *J Mol Biol* 275, 255-67.
- [13] Silver, F.H., Freeman, J.W. and Sehra, G.P. (2003) Collagen self-assembly and the development of tendon mechanical properties *J Biomech* 36, 1529-53.
- [14] Persikov, A.V., Ramshaw, J.A. and Brodsky, B. (2000) Collagen model peptides: Sequence dependence of triple-helix stability *Biopolymers* 55, 436-50.
- [15] Kramer, R.Z., Bella, J., Mayville, P., Brodsky, B. and Berman, H.M. (1999) Sequence dependent conformational variations of collagen triple-helical structure *Nature structural biology* 6, 454 - 457.
- [16] Kuznetsova, N., Chi, S.L. and Leikin, S. (1998) Sugars and polyols inhibit fibrillogenesis of type I collagen by disrupting hydrogen-bonded water bridges between the helices *Biochemistry* 37, 11888-95.
- [17] Mizuno, K., Hayashi, T., Peyton, D.H. and Bachinger, H.P. (2004) Hydroxylation-induced stabilization of the collagen triple helix. Acetyl-(glycyl-4(R)-hydroxyprolyl-4(R)-hydroxyprolyl)(10)-NH(2) forms a highly stable triple helix *J Biol Chem* 279, 38072-8.
- [18] Mizuno, K., Hayashi, T. and Bachinger, H.P. (2003) Hydroxylation-induced stabilization of the collagen triple helix. Further characterization of peptides with 4(R)-hydroxyproline in the Xaa position *J Biol Chem* 278, 32373-9.

REPORT DOCUMENTATION PAGE (SF298)
(Continuation Sheet)

- [19] Shoulders, M.D., Hodges, J.A. and Raines, R.T. (2006) Reciprocity of steric and stereoelectronic effects in the collagen triple helix *J Am Chem Soc* 128, 8112-3.
- [20] Hodges, J.A. and Raines, R.T. (2003) Stereoelectronic effects on collagen stability: the dichotomy of 4-fluoroproline diastereomers *J Am Chem Soc* 125, 9262-3.
- [21] Bretscher, L.E., Jenkins, C.L., Taylor, K.M., DeRider, M.L. and Raines, R.T. (2001) Conformational stability of collagen relies on a stereoelectronic effect *J Am Chem Soc* 123, 777-8.
- [22] Holmgren, S.K., Bretscher, L.E., Taylor, K.M. and Raines, R.T. (1999) A hyperstable collagen mimic *Chem Biol* 6, 63-70.
- [23] Hulmes, D.J. and Miller, A. (1979) Quasi-hexagonal molecular packing in collagen fibrils *Nature* 282, 878-80.
- [24] Kar, K., Amin, P., Bryan, M.A., Persikov, A.V., Mohs, A., Wang, Y.H. and Brodsky, B. (2006) Self-association of collagen triple helix peptides into higher order structures *J Biol Chem* 281, 33283-90.
- [25] Kramer, R.Z., Venugopal, M.G., Bella, J., Mayville, P., Brodsky, B. and Berman, H.M. (2000) Staggered molecular packing in crystals of a collagen-like peptide with a single charged pair *J Mol Biol* 301, 1191-205.
- [26] Valluzzi, R. and Kaplan, D.L. (2000) Sequence-specific liquid crystallinity of collagen model peptides. I. Transmission electron microscopy studies of interfacial collagen gels *Biopolymers* 53, 350-62.
- [27] Helseth, D.L., Jr. and Veis, A. (1981) Collagen self-assembly in vitro. Differentiating specific telopeptide-dependent interactions using selective enzyme modification and the addition of free amino telopeptide *J Biol Chem* 256, 7118-28.
- [28] Bann, J.G. and Bachinger, H.P. (2000) Glycosylation/Hydroxylation-induced stabilization of the collagen triple helix. 4-trans-hydroxyproline in the Xaa position can stabilize the triple helix *J Biol Chem* 275, 24466-9.
- [29] Bann, J.G., Peyton, D.H. and Bachinger, H.P. (2000) Sweet is stable: glycosylation stabilizes collagen *FEBS Lett* 473, 237-40.
- [30] Bann, J.G., Bachinger, H.P. and Peyton, D.H. (2003) Role of carbohydrate in stabilizing the triple-helix in a model for a deep-sea hydrothermal vent worm collagen *Biochemistry* 42, 4042-8.
- [31] Orgel, J.P., Wess, T.J. and Miller, A. (2000) The in situ conformation and axial location of the intermolecular cross-linked non-helical telopeptides of type I collagen *Structure* 8, 137-42.
- [32] Holmes, D.F., Graham, H.K., Trotter, J.A. and Kadler, K.E. (2001) STEM/TEM studies of collagen fibril assembly *Micron* 32, 273-85.
- [33] Tsao, T.S., Tomas, E., Murrey, H.E., Hug, C., Lee, D.H., Ruderman, N.B., Heuser, J.E. and Lodish, H.F. (2003) Role of disulfide bonds in Acrp30/adiponectin structure and signaling specificity. Different oligomers activate different signal transduction pathways *J Biol Chem* 278, 50810-7.
- [34] Tsao, T.S., Murrey, H.E., Hug, C., Lee, D.H. and Lodish, H.F. (2002) Oligomerization state-dependent activation of NF-kappa B signaling pathway by adipocyte complement-related protein of 30 kDa (Acrp30) *J Biol Chem* 277, 29359-62.

- [35] Pajvani, U.B. et al. (2004) Complex distribution, not absolute amount of adiponectin, correlates with thiazolidinedione-mediated improvement in insulin sensitivity *J Biol Chem* 279, 12152-62.
- [36] Pajvani, U.B. et al. (2003) Structure-function studies of the adipocyte-secreted hormone Acrp30/adiponectin. Implications for metabolic regulation and bioactivity *J Biol Chem* 278, 9073-85.
- [37] Wang, Y., Xu, A., Knight, C., Xu, L.Y. and Cooper, G.J.S. (2002) Hydroxylation and glycosylation of the four conserved lysine residues in the collagenous domain of adiponectin *J. Biol. Chem.* 277, 19521 - 19529.
- [38] Wang, Y. et al. (2006) Posttranslational modifications on the four conserved lysine residues within the collagenous domain of adiponectin are required for the formation of its high-molecular-weight oligomeric complex *J Biol Chem*.
- [39] Richards, A.A., Stephens, T., Charlton, H.K., Jones, A., Macdonald, G.A., Prins, J.B. and Whitehead, J.P. (2006) Adiponectin multimerisation is dependent on conserved lysines in the collagenous domain: Evidence for regulation of multimerisation by alterations in post-translational modifications *Mol Endocrinol* 20, 1673-1687.
- [40] Wang, Y., Lu, G., Wong, W.P., Vliegenthart, J.F., Gerwig, G.J., Lam, K.S., Cooper, G.J. and Xu, A. (2004) Proteomic and functional characterization of endogenous adiponectin purified from fetal bovine serum *Proteomics* 4, 3933-42.
- [41] Suzuki, S., Wilson-Kubalek, E.M., Wert, D., Tsao, T.S. and Lee, D.H. (2007) The oligomeric structure of high molecular weight adiponectin *FEBS Lett*.
- [42] Frisken, B.J. (2001) Revisiting the method of cumulants for the analysis of dynamic light-scattering data *Appl. Optics* 40, 4087-4091.
- [43] Laue, T.M., Shah, B.D., Ridgeway, T.M. and Pelletier, S.L. (1992), pp. 90-125 (Harding, S. and Rowe, A., Eds.) Redwood Press Ltd, Melksham, UK.
- [44] Liberti, P.A. and Paul, S.M. (1978) Gross conformation of C1q: a subcomponent of the first component of complement *Biochemistry* 17, 1952-8.
- [45] Strang, C.J., Siegel, R.C., Phillips, M.L., Poon, P.H. and Schumaker, V.N. (1982) Ultrastructure of the first component of human complement: electron microscopy of the crosslinked complex *Proc Natl Acad Sci U S A* 79, 586-90.
- [46] Slayter, H.S., Alexander, R.J. and Steiner, L.A. (1983) Electron microscopy of the complement protein C1q from the bullfrog, *Rana catesbeiana* *Eur J Immunol* 13, 102-6.
- [47] Pajvani, U.B. et al. (2003) Structure-function studies of the adipocyte-secreted hormone Acrp30/adiponectin. Implications for metabolic regulation and bioactivity *J Biol Chem* 278, 9073-85.
- [48] Waki, H. et al. (2003) Impaired multimerization of human adiponectin mutants associated with diabetes. Molecular structure and multimer formation of adiponectin *J Biol Chem* 278, 40352-63.

V. Publications and Technical Reports

a. Papers published in peer-reviewed journals:
Suzuki, S., Kubalek, E.W., Wert, D., Tsao, T.-S., Lee, D.H. "The Oligomeric Structure of High Molecular Weight Adiponectin" *FEBS Lett. In press (2007)*.

b. Papers published as conference proceedings:
Fu, X., Stubbs, G., & Lee D.H., "Self-assembly of a Linear Viral Array" conference proceedings of FNANO 2005, Snowbird Lodge, Utah.

c. Manuscripts submitted but not published:
Fu, X., Stubbs, G., & Lee D.H., "Self-Assembly of a Linear Viral Array", in revision.

d. Technical reports submitted to ARO
Interim progress reports were submitted in 2003, 2004 and 2005.

VI. Participating Scientific Personnel:

<u>Graduate Students</u>	<u>Project</u>	<u>Degree Earned</u>
Xiaorong Fu	TMV	M.Sc.
Michael Ramos	IF	M.Sc.
Jennifer Rego	TMV	currently a Ph.D. candidate
Shinji Suzuki	Adiponectin	currently a M.Sc. candidate
Postdoctoral Fellows		
Kuiyang Jiang, Ph.D.	TMV	N/A

VII. Report of Inventions

Provisional Application: Purified High Molecular Weight Adiponectin and Uses Thereof